Journal of Building Engineering 94 (2024) 109912

Contents lists available at ScienceDirect

Journal of Building Engineering

journal homepage: www.elsevier.com/locate/jobe

Encapsulation of sodium silicate to attain on demand buildability enhancement in concrete 3D printing

Sasitharan Kanagasuntharam [a], Sayanthan Ramakrishnan [b,*], Jay Sanjayan [a]

[a] Centre for Sustainable Infrastructure and Digital Construction, School of Engineering, Swinburne University of Technology, Hawthorn, Australia
[b] Centre for Future Materials, School of Engineering, University of Southern Queensland, Springfield Central, QLD 4300, Australia

ARTICLE INFO

Keywords:
Phase change material
Buildability
Set-on-demand
Encapsulated accelerators
Thermal intervention

ABSTRACT

This study investigates the encapsulation of a buildability enhancing additive using a phase change material (PCM) as a thermo-responsive additive for concrete 3D printing. The encapsulated additive is mixed with printable mixes and activated at the print head. The printhead activation via the heating process dissolves the capsules and releases the buildability enhancing additive to attain the required rheological properties for printing. A sodium silicate-based set accelerator was used as the buildability enhancing additive and encapsulated using a paraffinic PCM. The comprehensive experimental study was conducted to understand the effect of encapsulated sodium silicate on the pumpability of concrete followed by buildability after print head heating. It was demonstrated that the smaller addition of encapsulated sodium silicate (5 %) followed by print head activation resulted in the static yield strength (SYS) of 122 kPa after 25 min of placement compared to 8 kPa observed for mixes containing nanoclay as a thixotropic additive. Furthermore, the dissolution process of sodium silicate was assessed via an analytical method using optical technology to determine the diffusion coefficient of sodium silicate in the printable concrete. The proposed method was validated by printing a thin vertical wall with the optimised mix design developed during the study. Consequently, the mechanical properties of the printed specimen were investigated. The mixes containing the encapsulated additive showed a compressive strength reduction by up to 47 % for mould cast and 3D printed specimens and this was correlated to increased porosity of the mixes.

1. Introduction

Concrete 3D printing is an emerging digital construction technology that adopts robots and/or 3D printing machinery to place the fresh concrete layer by layer until the desired structure is built. This technique does not require formwork, therefore the concrete needs to exhibit contradicting rheological properties during printing. For instance, the concrete needs to exhibit low static yield stress and viscosity during pumping to have an extended operating duration, whereas the concrete after placement needs a rapid strength development rate for faster stacking of layers without excessive deformation or collapse. These contradictory rheological properties are achieved using various set on demand approaches: 1) Print head heating: The concrete with a long open time is pumped to the print head and heated before deposition. The heating increases the reaction kinetics of the concrete which in turn increases its strength development. The print head heating can be achieved using conventional coil heating, microwave radiations [1,2], water bath etc. 2) Inline addition of buildability enhancing additive: A stimuli-responsive buildability enhancing additive is added at the print head to

* Corresponding author.
E-mail address: Saya.Ramakrishnan@unisq.edu.au (S. Ramakrishnan).

https://doi.org/10.1016/j.jobe.2024.109912
Received 30 January 2024; Received in revised form 31 May 2024; Accepted 10 June 2024
Available online 11 June 2024

enhance the strength development rate after placement. This technique requires an in-line mixer which can be dynamic [3,4] or static [5]. Compared to other approaches, this is the most studied technique to attain an on-demand setting in printable concrete for both cementitious [6,7] and other binder systems [5]. However, the uniform mixing of the accelerator with the concrete is challenging with this method as the residence time of the concrete in the in-line mixer is short. To solve this problem, some studies have investigated the incorporation of encapsulated additives during the initial mixing stage and activation at the print head. The addition of encapsulated accelerators during the initial mixing allows uniform distribution of the additive. Furthermore, the encapsulation prevents the interaction of additives with the cement such that the concrete remains pumpable regardless of the additive dosage. The concrete with encapsulated additive is pumped to the print head and activated shortly before the deposition. The activation process, commonly conducted through print head heating, ensures the release of additive followed by the interaction with the binder in the printable mixes. The most commonly used additives were set accelerators in the form of shotcrete liquid accelerators, sodium hydroxide etc. This approach was previously investigated in Refs. [8–11]. Polyethylene glycol was employed to encapsulate additives designed to enhance buildability by Shao et al. [11]. Specifically, the study focused on a combination of set accelerators and viscosity-modifying agents, with a prescribed mass ratio of 9:1. Microwaves were used to heat the mixture at the print head, inducing controlled melting of the polyethylene glycol for a precise release of the additives. Given that concrete comprises dielectric components, the application of microwaves instigates heating through frictional losses within the mixture. This process generates heat and hence elevates the temperature of concrete, leading to the controlled rupture of the capsule shell [1,12,13]. In the study [11], researchers incorporated graphite powder, known for its microwave-absorbing properties, alongside buildability-enhancing additives to optimize the efficiency of microwave heating. This modification reduced the required microwaving duration for capsule shell melting, consequently diminishing the residence time of the concrete in the print head where heat is applied. The controlled release of accelerator was investigated by quantifying Cl-ions in the solution after microwave heating of water and cement paste. The results affirm that the capsules remain intact until reaching the print head, with the mix displaying controlled release of the accelerator post-print head heating. While the outcomes reported by Shao et al. [11] are promising, the application of microwave heating in large-scale concrete 3D printing is debatable, primarily due to workplace safety regulations. As an alternative, the heating of the print head can be achieved through safer methods, such as electrical coils, heating mats, or water baths. The choice of a suitable print head heating method becomes critical in ensuring a seamless and efficient 3D printing process while adhering to safety regulations.

In another study [9], sodium hydroxide (NaOH) was used as an additive and it was encapsulated using a phase change material (PCM) with a melting temperature of 31 °C. The results demonstrated that the NaOH additive led to the rapid setting of concrete after placement, however, it showed detrimental effects on the hardened properties of the concrete. In addition, the concrete with encapsulated NaOH requires a simultaneous heating and mixing process at the print head to activate the NaOH. Therefore, it was concluded that the NaOH may not be the best set accelerator for this purpose.

Concerning the promising outcomes achieved by the encapsulated additive method for the buildability enhancement of 3DCP mixes, this study investigates sodium silicate as an additive for buildability enhancement. In the presence of sodium silicate in concrete, dissolved Ca^{2+} ions from the cement react with sodium silicate to produce insoluble calcium silicate. The formation of insoluble calcium silicate increases the solid content of the mix, which in turn, increases the static yield strength of fresh printable mixes (buildability). Sodium silicate has been previously studied to accelerate the setting rate of cement, especially in oil-well cement [14–16]. However, its application to attain the on-demand setting of printable mixes is yet to be investigated. It is worth mentioning here that sodium silicate has relatively less solubility than sodium hydroxide. Therefore, the release of sodium silicate after print head heating might not provide an immediate increment in static yield strength like in the case of sodium hydroxide. On the other hand, excessive dosage of sodium silicate can significantly reduce the hardened properties of the concrete. Even though sodium silicate provides reactive silicate ions to the pore solution which enhances the formation of C–S–H, it also increases the pH of the pore solution which enhances the formation of ettringite. Therefore, this paper first investigates the effect of sodium silicate at various dosages on the fresh properties of the printable mix to identify the optimum dosage. This was followed by studying the diffusion rates of the accelerator into the fresh concrete after print head heating. This is to provide a comprehensive insight into both the mechanism of accelerator diffusion and the associated diffusion coefficient. Once a suitable dosage was identified, the proposed technology was validated by printing thin vertical print sections and studying the hardened properties of printed concrete.

2. Materials and methods

2.1. Materials

This study uses Ordinary Portland Cement (OPC) sourced from Cement Australia as the binder. The OPC, specified as general-purpose (GP) conformed to AS3972 standard [17]. Two distinct grades of sand, marked as coarse sand (CS) and medium sand (MS), were supplied by Holcim, Australia. To enhance the workability and extend the open time of the mixture, chemical admixtures of polycarboxylic ether-based superplasticizer (SP, MasterGlenium SKY 8379) and a retarder (MasterSet RT 122) were used respectively. Sodium silicate pellets (Na_2SiO_3) with a purity of 99 % were sourced from Redox Pty. Ltd., Australia. In this study, Na_2SiO_3 functioned as the set accelerator to improve the buildability of the 3D printable concrete [18–20]. The encapsulation of Na_2SiO_3 pellets was achieved using a thermo-responsive paraffinic Phase Change Material (PCM), RT32 from RUBITHERM®. RT32 exhibits a phase transition temperature of approximately 31 °C. Furthermore, the study conducts a comparative analysis between the proposed method of using encapsulated additives with the traditional buildability enhancement approach of incorporating thixotropic additives during the initial mixing stage. Nano clay, also known as Magnesium Alumino Silicate (MAS), supplied by Active Minerals International, LLC, was used as a thixotropic additive. Additional details about the specific nano clay can be found in Refs. [9,21]. The study with MAS was conducted to compare the traditional buildability enhancing approach with in-line activation using encapsulated accelerators. The

Table 1
Mix design of the materials used in this study.

Mix ID	Cement	Water/Cement ratio	Sand/Binder		WRA (g/kg of OPC)	Retarder (g/kg of OPC)	Accelerator dosage (g/kg of OPC)	heat applied	Nano clay (g/kg of dry mix)	Mixing after heating
			Coarse	Fine						
M	1	0.34	1	0.5	4.71	5	0	N	N/A	N
S-2							20	N		N
S-3.5							35	N		N
S-5							50	N		N
S-2HM							20	Y		Y
S-3.5HM							35	Y		Y
S-5HM							50	Y		Y
M-P							0	N	4	N

encapsulation process of the Na_2SiO_3 is similar to the encapsulation of NaOH pellets reported in Kanagasuntharam et al. [9].

2.2. Preparation of printable concrete

The mix design for the mixes used in this study is given in Table 1, where two distinct buildability enhancement strategies were investigated. First, print head heating of the mixture containing encapsulated Na_2SiO_3 was investigated to achieve on-demand improvement in buildability. Second, a thixotropic additive (nano clay) was introduced during the initial mixing stage to compare the traditional buildability enhancement technique (i.e., using the thixotropic additive) with the newly introduced encapsulated accelerator technique. These mixes are denoted as M, S-x and M − P for control mix without any buildability enhancement technique, mixes containing x amount of Na_2SiO_3 and mix containing thixotropic additive respectively. The mixes incorporating encapsulated additive contain Na_2SiO_3 at dosages ranging from 0 wt% to 5 wt% of cement. The suffixes "H" and "M" in the mixes with encapsulated additive (S-x) denote print head heating and print head mixing, respectively. For example, Mix S-2 corresponds to the mix with 2 % of encapsulated Na_2SiO_3 with neither print head heating nor mixing processes and mix S-2HM represents 2 % additive with simultaneous print head heating and mixing. For all mixes, the ratio between cement and sand was maintained at 1.5, and the dosages of superplasticizer (SP) and retarder were consistently set at 4.71 and 5 g/kg of OPC, respectively. In Mixes S-2 and S-5, the Na_2SiO_3 dosage was varied from 2 wt% to 5 wt% to assess its impact on the fresh and hardened properties of the printable mix. The nano clay dosage in Mix M − P was fixed at 0.4 wt% based on preliminary studies, as further additions showed significant challenges in pumping and extrusion processes.

The mixing method involved a sequence of steps. First, the dry components (sand and cement) were added to the mixing bowl and stirred for 1 min at 61 RPM. Simultaneously, a solution of water, superplasticizer (SP), and retarder was prepared according to the mix design in Table 1. The prepared solution was gradually added after dry mixing, and mixing was carried out for 2 min at 125 RPM. Subsequently, wet mixing was briefly paused to scrape materials adhered to the sides and bottom of the mixing bowl and blades, ensuring homogeneous mixing. Wet mixing was then resumed for 1 min at 61 RPM. The fabricated capsules were then added to the wet cementitious mix at a predetermined dosage and stirred for 30 s at 61 rpm. To simulate print head heating, the blended cementitious mix with encapsulated Na_2SiO_3 was immersed in the water bath for 30s at the water temperature of 65 °C with simultaneous mixing for mixes requiring heating and mixing. This heating process is anticipated to melt the encapsulation, releasing Na_2SiO_3 to enhance the buildability of the printed layer. For the validation using a prototype printing, a heating system with water circulated at 65 °C was fabricated at the laboratory and used as explained in section 2.3.

2.3. Experimental methodology

2.3.1. Static yield strength (SYS) evolution with time

The evolution of the static yield strength (SYS) for the proposed mixes was assessed using a slow penetration test. Following the in-line activation of the concrete (via print head heating with mixing), the mixture was transferred to a sample cup with dimensions of 80 mm in diameter and 120 mm in height. A conical needle connected to a 500 N load cell, was gradually penetrated into the fresh concrete. The penetration rate was controlled at 10 mm/h using a displacement-controlled compression loading setup in a Mechanical Testing System (MTS) machine. The load cell continuously recorded the resistance to penetration, which was used to calculate the SYS using the formula given below [22,23]:

$$\tau = \frac{F}{\pi R\sqrt{R^2 + h^2}} \quad \text{Eq(1)}$$

Where, τ and F represents the SYS and penetration resistance respectively. R and h are the radius and height of the conical needle.

2.3.2. Elastic modulus of the printed layer

Both the stiffness of the printed layer and the SYS have an impact on the printable mix's buildability. The SYS and its evolution over time govern buildability failure due to plastic collapse, while the stiffness evolution of the filament improves the stability against the elastic buckling failure during printing. To characterize stiffness, the elastic modulus of the printed layer was measured at various rest times after printing (ranging from 10 to 40 min) [24]. Freshly prepared concrete was transferred to a customized 3D printer, which was used to print two-layered specimens measuring 200 mm in length, 40 mm in width, and 40 mm in thickness. Fresh concrete is held in a

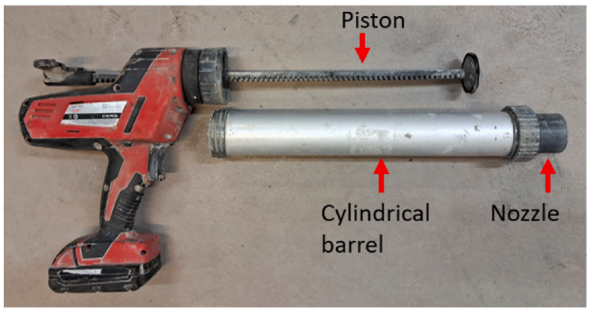

Fig. 1. A customised 3D printer consists of a piston-type extruder.

1.2-L cylindrical barrel that is attached to a piston-type extruder in the piston 3D printer as shown in Fig. 1. To regulate the shape of the extruded filament, the barrel's opposite end is attached to a rectangular nozzle that measures 40 mm in width and 20 mm in height. After printing, the specimens were kept in a temperature and humidity-controlled environment operated at 25^0 C and 50 RH% until testing. The printed specimens were then subjected to compression loading using the MTS machine at a displacement-controlled loading rate of 10 mm/min. A 10 kN load cell that was mounted on the machine was used to measure the applied load. The resulting load vs. displacement data was converted into a stress vs. strain graph, and the printed layer's elastic modulus was derived by calculating the slope of the linear component of the graph up to 5 % strain. It's important to note that since the printed specimens were in a fresh state, axial deformation occurrs during unconfined compression. As a result, the cross-sectional area under load continuously changed during the test. However, the variations in cross-sectional area in the measurement zone were negligible since the elastic modulus was found within the linear section up to the 5 % strain limit. Additionally, any error introduced by variations in cross-sectional area would be consistent across all specimens, as the results were utilized for comparing the stiffness of various mixes.

2.3.3. Mini-slump test

Prior to print head activation, a mini slump test was carried out as per ASTM C1437 [25] to evaluate pumpability characteristics. In this experiment, all mixes prior to print head heating were added to a truncated mini-slump cone measuring 70 mm in the top radius, 100 mm in the bottom radius, and 100 mm in the height. The cone was raised to measure the spread diameter of the fresh mix. The mini-slump test was conducted at 10 min intervals to evaluate the slump loss with time. To compare the pumpability of the proposed method with the traditional method by using a thixotropic additive, the spread diameter variation over time for the mix with nano clay was also determined.

2.3.4. Diffusion rate of encapsulated additive after activation

To evaluate the diffusion rate of encapsuled additive after activation, the concrete was prepared using a white cement, which shared the same grade and properties as the ordinary Portland cement used in the previous sections. To facilitate the tracking of sodium silicate's diffusion through the white concrete, the accelerator was doped with the black colour pigments and then encapsulated with PCM. It is important to emphasise that the overall mix composition of white concrete used in this study is consistent with the formulation of Mix M used in the previous sections. The incorporation of black pigments into the sodium silicate and the encapsulation within paraffinic PCM - RT32 from RUBITHERM® serves the dual purpose of providing visual tracking and ensuring that the experimental method aligns with the proposed set-on-demand approach. To investigate the release and diffusion of the encapsulated

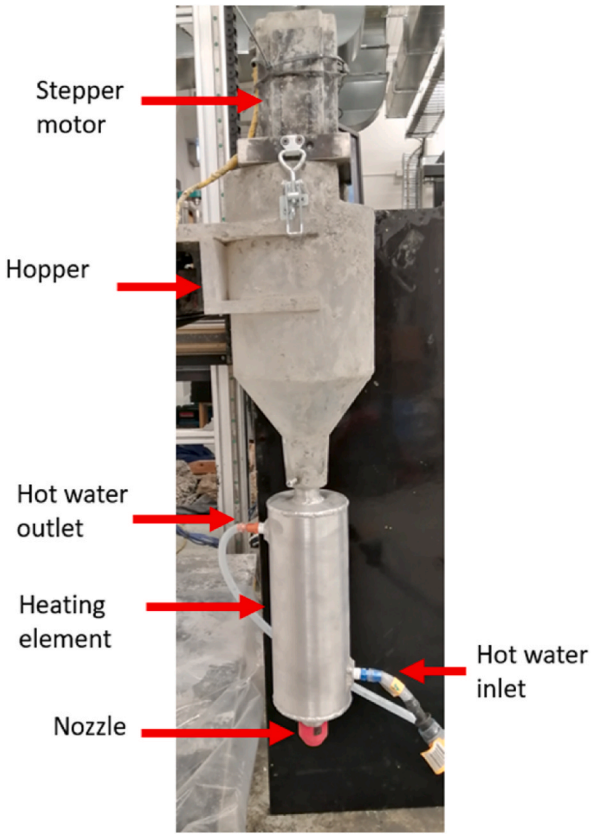

Fig. 2. The print head setup used to attain an on-demand setting in concrete for 3D printing (Image reproduced from Ref. [9]).

black coloured sodium silicate accelerator within the concrete under conditions simulating print head heating, a cylindrical glass container of 150 mm diameter and 100 mm height was utsed. Fresh concrete, prepared using the white cement, was poured into the container. In the centre of the container, the encapsulated accelerator was partially immersed in the fresh concrete. It is worth noting that under actual print head heating conditions, the capsule would be fully immersed in the fresh concrete. However, for the purposes of effective tracking, the encapsulated sodium silicate was partially immersed. The container was subsequently placed in a temperature-controlled water bath set at 60 °C. The release and diffusion of the accelerator were captured using a high-resolution camera. Video footage was acquired and subsequently analysed by extracting images at predefined time intervals. Through a detailed visual analysis of these images, the diffusion coefficient was determined.

2.3.5. Prototype development and printing validation

In this section, three mixes of M − P (with nano clay), S-3.5HM and control mix (M) with heating were printed for validation of the studied set-on-demand method (i.e., the print head heating of the concrete blended with encapsulated sodium silicate). It is worth mentioning here that the mix S-5HM was not used for the validation because of the high dosage of encapsulated sodium silicate in the mix. The mix S-5HM was removed from the validation section since there were still undissolved capsules visible on the printed layer's surface. This is because, for the print head configuration used in this experiment, the concrete's residence duration in the heating zone is insufficient to melt every capsule in the mix S-5HM. Meanwhile, the mix M − P was selected to understand the effect of thixotropic additive (commonly used strategy) on the buildability enhancement of 3D printable concrete. In the case of mixes with sodium silicate, mix S-3.5HM (3.5 wt% sodium silicate dosage) was selected as the optimum mix design. The proposed set-on-demand method will use heating at the print head to dissolve the encapsulation. This heating could also accelerate the SYS development of concrete. Therefore, the control mix (M) was also subjected to a heating process at the print head to study the buildability enhancement with Na_2SiO_3 only. The set-on-demand strategy with encapsulated sodium silicate involves print head heating. Heating accelerates the hydration reaction kinetics, resulting in enhanced buildability. Therefore, mix M (i.e., mix S-3.5HM without encapsulated sodium silicate) was also heated at the print head before the deposition. For clarity, the mix M after heating will be referred to as M − H hereafter. Printing with the mix M − H will determine the influence of heating in the studied set-on-demand approach. For instance, if the difference in failure height between the heated mixes containing encapsulated sodium silicate and without encapsulated sodium silicate is insignificant, it implies that the buildability enhancement is majorly due to heating.

Hot water was circulated around the print head to heat the mixes before the deposition as shown in Fig. 2. The hot water was continuously pumped from the reservoir using a FASCO evaporative cooler pump at a rate of 25 ml/s. The hot water after heating the concrete was transferred back to the reservoir where the temperature was maintained at 65 °C. The print head also consisted of a hopper (attached above the heating system) where the mix was introduced to the print head. A screw extruder was used for transporting the concrete from the hopper to the nozzle via the heating system.

2.3.6. Mechanical properties of concrete containing encapsulated Na_2SiO_3 additives

To evaluate the impact of encapsulated Na_2SiO_3 additives on the mechanical properties of concrete mixes, the compressive strength of both mould-cast and 3D-printed specimens was assessed. The mixes (post-print head activation) were filled into steel moulds measuring 50 x 50 × 50 mm^3, and they were compacted using a mechanical vibrator to produce the specimens. After the mould-cast procedure, the moulds were sealed and allowed to cure for a day at room temperature. The specimens were demoulded and kept in a water bath until the testing date following this sealed curing time. The cubes were taken out of the water bath on test day and subjected to compressive strength test. A loading rate of 0.33 kN/s was maintained for all specimens. For every mix design, three cubes were tested, and the average compressive strength is reported with one standard deviation.

To compare the compressive strength of the 3D-printed specimens with their mould-cast equivalents, the fresh printable mixtures were 3D printed concurrently once the print head heating was activated. Due to the anisotropic properties of the printed specimens, the compressive strength was determined for three loading directions: longitudinal, lateral, and perpendicular [26]. A two-layered prism measuring 200 mm in length, 40 mm in width, and 40 mm in thickness was printed using a customised 3D printer described earlier. The printed specimens were then sealed and cured for 24 h. Subsequently, they were subjected to further curing in a water bath until the test date. The prisms were cut into 40 mm × 40 mm x 40 mm cubes on the test date to assess their compressive strength. Each mix design and loading direction was tested with three cubes, and the average result was reported along with one standard deviation.

The interlayer bond strength was assessed by testing 40 x 40 × 40 mm^3 specimens extracted from two-layered prisms (200 mm × 40 mm x 20 mm) created using the custom 3D printer. A specialized metallic brackets connected to a universal MTS machine was used for the interlayer bond strength test, as described in a previous study [27]. To ensure the failure plane occurred at the interlayer, a 4 mm triangular notch was introduced on both sides of the interlayer. This notch not only facilitated the failure at the desired plane but also assisted in the secure placement of the samples onto the metallic brackets. The tests were conducted using a displacement control method at a rate of 0.5 mm/s. Three samples were tested for each group, and the average interlayer bond strength, along with one standard deviation, was reported.

2.3.7. Apparent volume of permeable voids test

The apparent volume of permeable voids (AVPV) test was conducted for mixes with varying Na_2SiO_3 dosages and nano clay for both mould-cast and printed specimens, following the procedures outlined in ASTM C642 [28]. In this test, the specimens were heated to 105 °C until a constant weight was reached, at which point their original oven-dry weight (w1) was determined. The samples were then submerged in boiling water for 5 h, and the mass of the specimens that had surface-dried was calculated as w2. Lastly, a metallic cage was used to suspend the samples in water, and the suspended weight was measured as w3. The AVPV was determined using Equation (2). Three specimens were tested and an average AVPV with one standard deviation was reported.

$$AVPV = \frac{w2\text{-}w1}{w2\text{-}w3} \times 100\% \quad \text{Eq(2)}$$

3. Results and discussion

3.1. Effect of sodium silicate dosage on the fresh properties of the mix

3.1.1. Flow table test

Fig. 3 shows the effect of sodium silicate dosage on the spread diameter of the fresh concrete. It was found that the increment in the sodium silicate dosage decreases the initial spread of the concrete. However, the rate of reduction in the spread diameter was found to be similar for all the sodium silicate dosages. For instance, the mix S-2 (dosage of 2 wt%) exhibited an initial spread of 206 mm and the spread was reduced by 14 % after 45 min of mixing. Similarly, in the case of mix S-3.5 and mix S-5, the initial spread was determined as 190 mm and 174 mm respectively. After 45 min of mixing, the spread was reduced by 15 % and 19 % for the mix S-3.5 and S-5 respectively. Most likely, the increment in the sodium silicate dosage introduces more microcapsules to the system, which in turn increases the total solid contents in the mix. This reduces the initial spread as shown in Fig. 3. Meanwhile, as the sodium silicate is encapsulated, its effect on the hydration of the cement paste was minimal, which could be seen in the rate of change in the spread diameter of printable concrete with varied sodium silicate dosages.

When the concrete was heated followed by mixing, the capsules were dissolved, and the sodium silicate was released into the matrix. Therefore, the sodium silicate reacted with cement and significantly reduced the spread of the concrete. Regardless of the sodium silicate dosage, when the concrete was heated and mixed, it showed zero slump. The mix M − P with nano clay was also tested for the mini-slump test. As shown in Fig. 3, the mix M − P showed no spread similar to the mixes with encapsulated sodium silicate after heating and mixing. Meanwhile, it is worth mentioning here that before the application of heating and mixing, the concrete with sodium silicate capsules showed good pumpability characterised by the spread.

3.1.2. SYS development with time

As the results from the flow table test did not clearly differentiate between the buildability of mixes with nano clay (traditional buildability enhancing approach) and encapsulated sodium silicate, the SYS development with time of the mixes was determined using a continuous penetration test. As shown in Fig. 4, the mixes that do not follow heating and mixing showed very low SYS growth with time. Similar observations were also made in the flow table test described in the previous section. After heating and mixing, the concrete with encapsulated sodium silicate showed a rapidly increasing SYS with time. For sodium silicate dosage of 2 wt%, the static yield after 25 min was 4.1 kPa when the concrete was not heated, whereas, after heating and mixing, the concrete exhibited a SYS of around 38 kPa (~10 times increment). Similarly, for the mix with 3.5 wt% sodium silicate dosage, the concrete exhibited a SYS of around 5.2 kPa, whereas after heating and mixing the concrete exhibited a SYS of around 79.5 kPa (¬ 14 times increment). Therefore, it can be implied that the increment in the SYS of the concrete after heating and mixing was governed by the sodium silicate dosage. The highest SYS development was observed for the mix with 5 wt% sodium silicate dosage. After 25 min from the first contact with water, the SYS was determined as 5.5 kPa, however, with the dissolution of the capsule with the heating and mixing, the 25 min SYS of the concrete was determined as 122 kPa.

It is worth mentioning here that the differences in the SYS development of the mixes with varied encapsulated sodium silicate dosages before heating are negligible compared to the difference in the SYS development of the mixes after heating and mixing. This implies that the addition of encapsulated sodium silicate has a negligible effect on the pumpability of the concrete when compared to the buildability of the concrete. Meanwhile, in the case of the mix M − P, the SYS development with time was faster than the mixes with

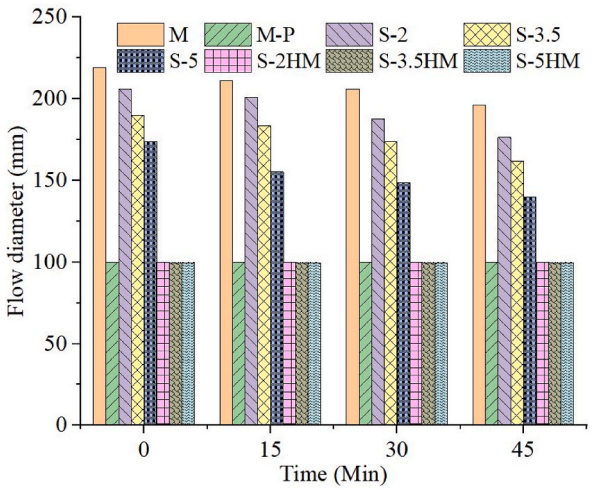

Fig. 3. Flow of the mixes with nano clay and various dosages of sodium silicate as buildability enhancing additives.

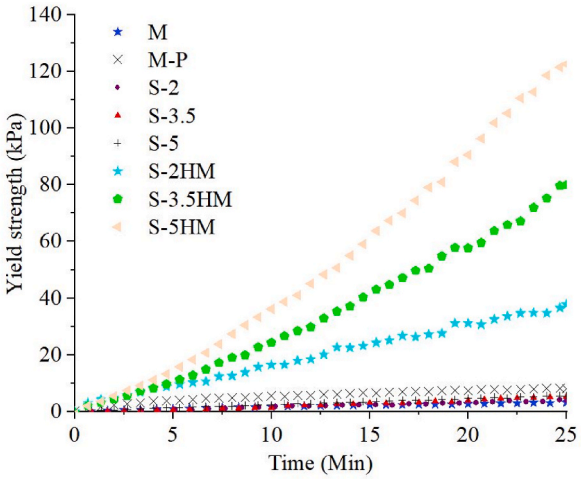

Fig. 4. SYS development with time of the mixes under investigation.

encapsulated sodium silicate without heating and mixing. For instance, the SYS of the mix M − P after 25 min was 8 kPa, whereas the SYS of the mixes S-2 (2 wt% dosage), S- 3.5 (3.5 wt% dosage) and S-5 (5 wt% dosage) was determined as 4.1 kPa, 5.2 kPa and 5.5 kPa. respectively. According to Muthukrishnan et al. [21], an SYS of above 5 kPa results in discontinuous printing. That means the mix with nano-clay has an open time of less than 15 min. It implies that the buildability enhancement achieved by the addition of a thixotropic additive (nano clay) is constrained by pumpability/extrudability limitations. However, in the case of mixes with encapsulated sodium silicate, the SYS remained less than 6 kPa throughout the testing duration regardless of the dosage. This translates to the concrete having better open time than the mix with nano clay.

3.1.3. Elastic modulus development with time

The buildability failure in concrete is due to a combined effect of plastic collapse and elastic buckling. The failure due to plastic collapse during printing is governed by the SYS and its evolution with time. In the case of elastic buckling, the failure is governed by the stiffness of the concrete, which is characterised by the modulus of elasticity. In addition, the stiffness is also related to the shape and size of the concrete specimen. Therefore, to investigate the effect of encapsulated sodium silicate on the buildability failure due to elastic buckling, the evolution of stiffness with time was determined for the printed layer.

Fig. 5 shows the elastic modulus of the printed layer at various resting durations ranging from 0 to 40 min. Similar to SYS results, the elastic modulus was found to increase with the increment in the sodium silicate dosage. For instance, the mix with 2 wt% of sodium silicate after heating and mixing showed an elastic modulus of 3380 kPa at 40 min, whereas the mix with 5 wt% of sodium silicate after heating and mixing showed an elastic modulus of 6293 kPa at the same time (40 min). Meanwhile, for the mix M − P, the elastic modulus was determined as 916 kPa at 40 min. Moreover, the development of elastic modulus with time for the mix with nano clay (mix M − P) was gradual compared to the rapid elastic modulus development for the mixes with the encapsulated sodium silicate. For instance, the elastic modulus of the mix M − P at 10 min residence time was determined as 484 kPa, which increased to 638 kPa after 20 min and 916 kPa after 40 min. In the case of the mix S-3.5 HM, the elastic modulus was determined as 1699 kPa after 10 min, which

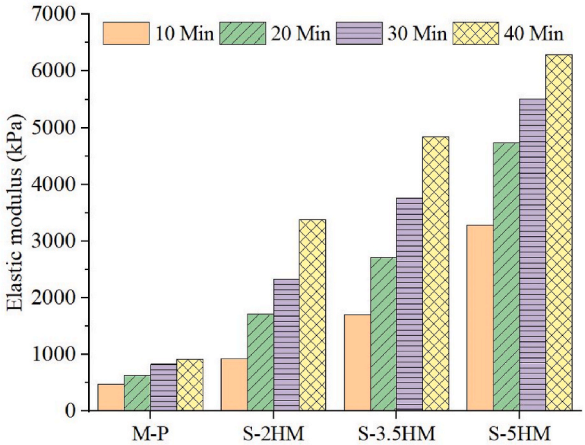

Fig. 5. Stiffness of the layer printed using the mixes with nano clay and sodium silicate as buildability enhancing additives.

rapidly increased to 2717 kPa after 20 min and 4843 kPa after 40 min. This implies that the mixes with encapsulated sodium silicate showed better resistance to the buildability failure mode – elastic buckling than the mixes with nano clay as the buildability-enhancing additive. Therefore, it can be concluded from previous sections that the encapsulated sodium silicate is a better buildability-enhancing strategy than nano clay in terms of resistance towards both the buildability failure modes - plastic collapse and elastic buckling. It is worth mentioning here that although the mixes with nano clay and encapsulated sodium silicate provided a similar spread, there was a substantial difference in the SYS and elastic modulus of the mixes. Therefore, it is necessary, especially for rapid hardening mixes, to conduct the SYS and elastic modulus tests to understand the buildability of the mixes.

3.2. Diffusion coefficient of sodium silicate in the concrete after print head heating

The viability of using encapsulated accelerators to accomplish on-demand setting in 3D concrete printing by means of print head heating was demonstrated in earlier sections. An examination was conducted to determine the impact of sodium silicate, the accelerator, on the properties of set-on-demand printable concrete, both in its fresh and hardened states. An increase in the sodium silicate dosage was shown to improve the concrete's stiffness and SYS. The mechanism of capsule melting during print head heating and the subsequent release of the accelerator, sodium silicate, into the cement matrix were identified as the causes of this effect. This section presents the experimental investigation of the diffusion coefficient which can be used for the mathematical modelling of the proposed print head heating method. Fig. 6 shows the partial immersion of dyed capsule containing the sodium silicate accelerator prior to the activation, whereas Fig. 7 illustrates the schematic diagram of the activation process.

The recorded observations unveiled a critical point in the process as shown in Fig. 8. After approximately 30 s of heating, the capsule initiated its melting process, leading to the significant release of the dyed sodium-silicate accelerator. Therefore, this was noted as 'time zero' for the subsequent evaluation of diffusion coefficients. Furthermore, a 10-s interval after 'time zero' (equivalent to 40 s from the initiation of heating) was chosen as the 'final time' for the diffusion coefficient assessment. This timeframe was critical for evaluating the extent of sodium silicate diffusion within the white concrete. As depicted in Fig. 8, two frames were extracted from the recorded video at the 30-s (representing the start of diffusion) and the 40-s mark (reflecting the diffusion's status after 10 s). Fluid diffusion into a porous medium is frequently described by Darcy's equation (Equation (3)). In this instance, the porous medium and diffusion fluids are white concrete and dyed sodium silicate accelerator respectively [29–32]. In the equation, C and D represent the concentration of the dyed sodium silicate accelerator and diffusion coefficient respectively. t corresponds to the time duration for the diffusion of the dyed sodium silicate accelerator, and x denotes the distance over which the dyed sodium silicate accelerator has diffused. This equation defines the process of natural diffusion of the sodium-silicate accelerator into the white concrete. That means this equation is suitable for characterizing the unassisted movement of the accelerator through the white concrete. Therefore, the encapsulated sodium silicate accelerator and the white concrete remained at rest throughout the entire duration of the experiment. This ensures that the diffusion process is not influenced by any forced diffusion mechanisms, such as mixing or agitation of the white concrete. Therefore, Darcy's equation is valid for the quantification of the natural diffusion of the sodium-silicate accelerator in our experimental setup.

As stated earlier, to determine the diffusion coefficient of the dyed sodium silicate accelerator within the white concrete, two snapshots extracted from the recorded video, taken at 30 s and 40 s from the onset of heating, were used for the analysis. The time taken for the concrete to reach from print head to the print bed was calculated as 30 s with the following printing parameters: Print head volume – 3 L, printing speed 100 mm/s, layer width - 50 mm, thickness −20 mm. These images were initially converted into greyscale to facilitate the quantification of black colour intensity within the white concrete along a defined axis. The partial differential equation (Darcy's equation) was transformed into a polynomial equation, as shown in Equation (4). This polynomial equation forms the basis for our analysis and the subsequent determination of the diffusion coefficient. The diffusion distance along the axis of interest was divided into 100 intervals, creating discrete segments of equal lengths. At each of these intervals, the intensity of the black colour within the white concrete was measured and recorded as C_1, C_2, C_3, and so forth up to C_5. These measured black colour intensity values, corresponding to the 6 intervals along the axis, were subsequently used to solve the polynomial equation (shown as Equation (4)) to calculate the diffusion coefficients. For example, C_1, C_2, and C_3 were individually substituted into Equation (2), yielding a diffusion

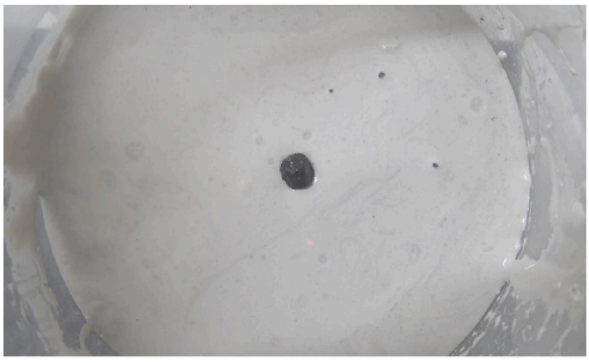

Fig. 6. Partial immersion of encapsulated dyed sodium silicate accelerator to experimentally validate the underlying mechanisms involved in the studied set-on-demand approach for buildability enhancement in concrete 3D printing.

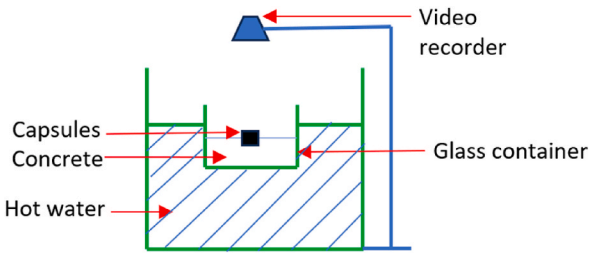

Fig. 7. Schematic representation of the experimental setup used to determine the diffusion coefficient.

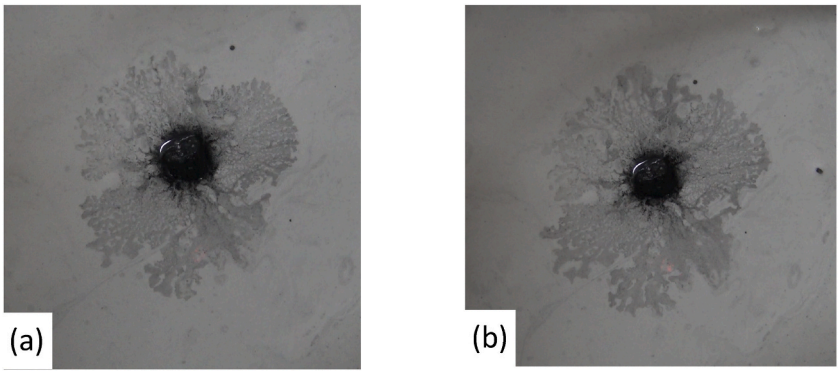

Fig. 8. Diffusion of dyed sodium silicate after (a) 30 s and (b) 40 s of heating with 60^0 C water bath.

coefficient D_1. Similarly, C_2, C_3, and C_4 were used to determine diffusion coefficient D_2, and this process was continued for all the consecutive intervals along the axis of interest. Here the points for the axis of interest were chosen between 3 mm (edge of the capsule) to 8 mm (end of the black colour diffusion) with 1 mm interval. An average grey scale value for each point was calculated by ring method as shown in Fig. 9. For instance, the grey scale value for the point at 4 mm from the capsule is determined by calculating the average grey scale value for the area between 3.5 mm and 4.5 mm radius ring. The result of this analysis indicated that the median diffusion coefficient was 0.04 mm^2/s. It is important to note that the diffusion coefficient will likely increase by many folds with the assistance of mixing or other forced diffusion techniques. This comprehensive assessment of diffusion coefficients at multiple points along the axis provides valuable insights into the diffusion of the sodium silicate accelerator into the concrete after heating. This in turn enhances our understanding of the in-line activation of printable concrete using print head heating of encapsulated accelerator to attain an on-demand setting for 3D concrete printing.

Fig. 10 depicts the concentration gradient of the Na_2SiO_3 with the distance from the capsule at 30 s and 40s from the diffusion initiation. As can be seen in Fig. 10, from 30s to 40s, the concentration of Na_2SiO_3 reduces up to 5 mm from the centre and increases beyond 5 mm. This indicates the diffusion of the Na_2SiO_3 with time. Moreover, the Darcy co-efficient determined by this method can be used in the mathematical model for 3D printing to determine the minimum threshold needed to achieve uniform accelerator diffusion in the concrete matrix. It guarantees that the set-on-demand can be accomplished efficiently with the fewest number of capsules. The coefficient can also used in 3D printing mathematical models to predict the failure layer height of structures[32].

$$\frac{\partial C}{\partial t} = D_{eff}\frac{\partial^2 C}{\partial x^2} \qquad \text{Eq(3)}$$

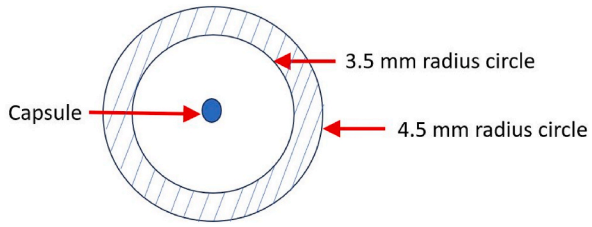

Fig. 9. Example schematic diagram of determining the average grayscale value at a distance 4 mm from the capsule.

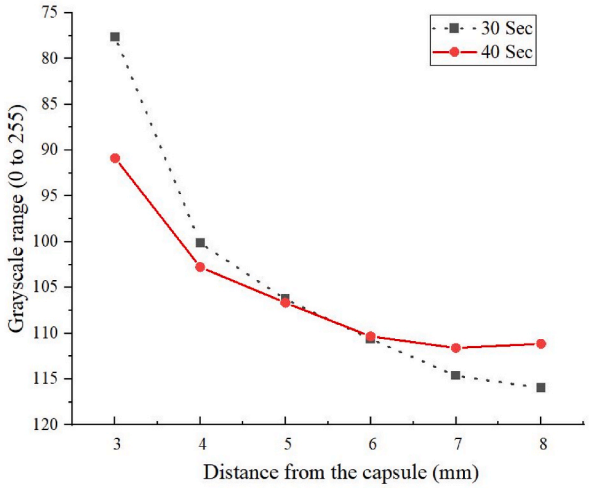

Fig. 10. The concentration gradient of the accelerator after 30 and 40 s of heating.

$$\frac{C_2(t+\Delta t)\text{-}C_2(t)}{\Delta t} = D_2\left(\frac{C_3(t)\text{-}2C_2(t)+C_1(t)}{(\Delta x)^2}\right) \quad \text{Eq(4)}$$

Where Δx is the distance between any two points.

3.3. Validation by printing

The printing validation was performed by depositing a 10 mm wide and 100 mm long layer one over the other until failure. The printing speed and the cycle time were maintained as 10 mm/s and 10 s respectively for all the mixes. Fig. 11 shows the printing of various 3D printable mixes developed in this study at the failure stage. As can be seen from Fig. 11, the mix M − P failed after printing 11 layers, whereas the mix S-3.5HM only failed after stacking 41 layers. Therefore, it can be concluded that the proposed set-on-demand approach provided better buildability enhancement than the thixotropic additives. The failure height of the mix M − H was determined as 8 layers compared to the 2 layers when the same mix was printed without heating (mix M). This implies that the print head heating influences the buildability enhancement achieved by the studied set-on-demand approach. Nevertheless, the significant contribution was from the encapsulated sodium silicate which can be justified by the determined failure height of the mix S-3.5HM (41 layers).

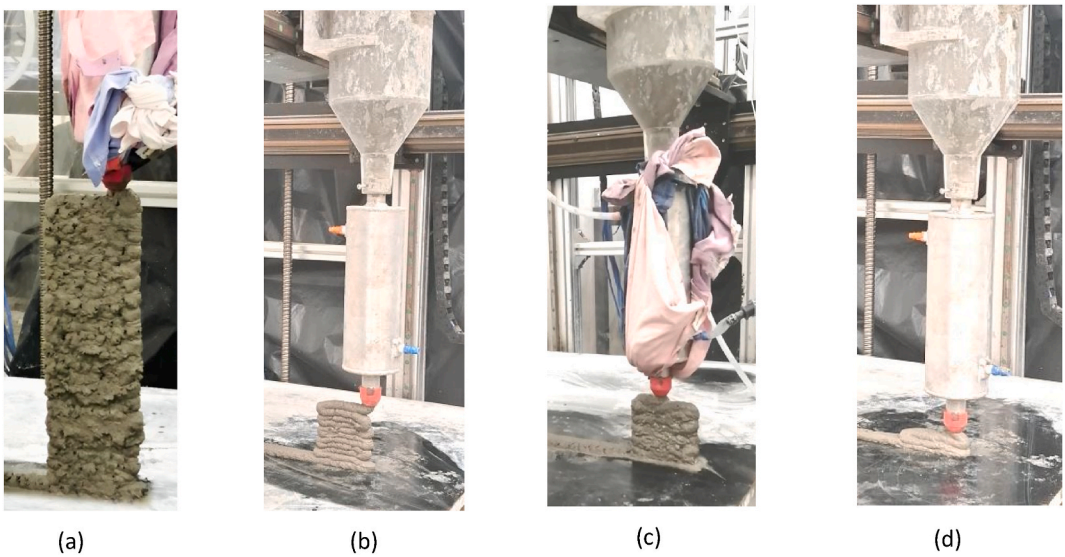

Fig. 11. Validation by printing using (a) Mix M − 3.5HM (41 layers), (b) Mix M − P (10 layers), (c) Mix M − H (8 layers) and (d) Mix M (2 layers).

3.4. Effect of sodium silicate dosage on the hardened properties of the mix

3.4.1. Compressive strength

Previous sections concluded that the addition of encapsulated sodium silicate during the initial mixing stage followed by print head heating and mixing provides significant enhancement in fresh properties of the concrete required for 3D printing application. As the concrete is developed for the construction industry, it is vital to understand the effect of observed buildability enhancement on the hardened properties of the concrete. Therefore, the 7- and 28-day compressive strength of the mixes was determined using the cast and printed specimens. Fig. 12 shows the compressive strength of the cast specimens, whereas Fig. 13 (a & b) shows the compressive strength of the printed specimen. As one could notice from these figures, the mould cast specimens showed higher compressive strength than the printed specimens regardless of the mix design. For instance, the mix M − P showed the compressive strength of 52 MPa and 66 MPa after 7 and 28 days from mould casting, whereas the specimens printed with the mix M − P showed the compressive strength of 36 MPa (~31 % reduction) and 43 MPa (~35 % reduction) at 7 and 28 days. The compressive strength determined during the perpendicular direction of loading (strongest direction) was used for the assessment. Similarly, the 7–day compressive strength of the printed specimen for 2 wt%, 3.5 wt% and 5 wt% of the sodium silicate dosage was 33 %, 37 % and 40 % lower than the mould cast specimens respectively, whereas the 28–day compressive strength of the printed specimen was 37 %, 41 % and 35 % lower than the mould cast specimens respectively.

Interestingly, the difference in the 7 and 28-day compressive strength reduced with the increment in the sodium silicate dosage. At 2 wt% of sodium silicate, the difference in the 7 and 28-day compressive strength was determined as 20.3 %. In the case of 5 wt% of sodium silicate dosage, the difference in the 7 and 28-day compressive strength was reduced to 10.1 %. Meanwhile, the difference in the 7 and 28-day compressive strength of the mix without any sodium silicate was 19.5 %. However, with the addition of nano clay, the compressive strength of the hardened specimens was not only higher than the sodium silicate specimens, but the increment in the compressive strength from 7 to 28 days was also larger. The difference in 7-day and 28-day compressive strength of the mix M − P was determined as 26.1 % which is 58 %, 116.6 % and 325.9 % higher than the mixes with 2 wt%, 3.5 wt% and 5 wt% sodium silicate dosages respectively. Nevertheless, it should be noted that all the mixes showed sufficient strength to be used as a building material in the construction industry.

Fig. 13(a and b) shows the compressive strength of the printed specimen prepared using mixes with nano clay and sodium silicate as the buildability-enhancing additives. Unlike the trend reported in Refs. [21,33], the printed specimens loaded in a perpendicular direction showed higher compressive strength than the other two directions. After the perpendicular direction, the specimens showed better compressive strength in a longitudinal direction. Hence, the specimens were weakest in the lateral direction regardless of the age and mix design. Most likely, it is due to the printing method followed in this study. As discussed before, the concrete after heating and mixing was deposited in two layers to obtain the specimens for testing. Moreover, the gap between the nozzle and the top surface of the previous layer was 1.5 times the layer thickness to ensure the effect of layer pressing on the interlayer bond strength was minimal. The interlayer formed in such a printing method is likely to be weak and reduces the compressive strength, especially in the longitudinal and lateral loading directions. In these directions, the load is applied in line with the interlayer, whereas in the case of perpendicular direction, the load applied is perpendicular to the interlayer. The reason behind the higher performance of the printed specimen in the longitudinal direction than in the lateral direction is the extrusion pressure. According to Arunothayan et al. [33], fresh concrete is compacted in the longitudinal direction due to the extrusion pressure, resulting in dense packing and, hence higher compressive strength in the longitudinal direction. The highest reduction in compressive strength from perpendicular to lateral loading direction was observed for the mix M-P. The reduction in 7-day compressive strength for the mix M − P, when the loading direction was changed from perpendicular to lateral direction, was determined as 30 %. the corresponding reductions for mixes S-2HM, S-3.5HM and S-5HM in 7-day compressive strength was determined as 28 %, 14 % and 26 % respectively. Although the reduction in compressive strength with the change in loading direction was highest for the mix with nano clay, it showed higher compressive strength than the mixes with

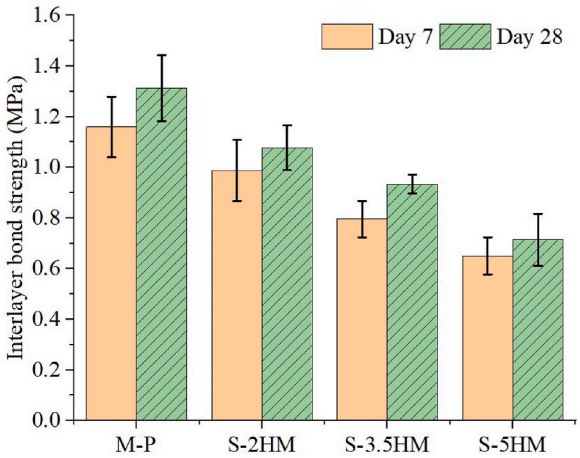

Fig. 12. 7 and 28-day compressive strength of the cast specimens developed using mixes under investigation.

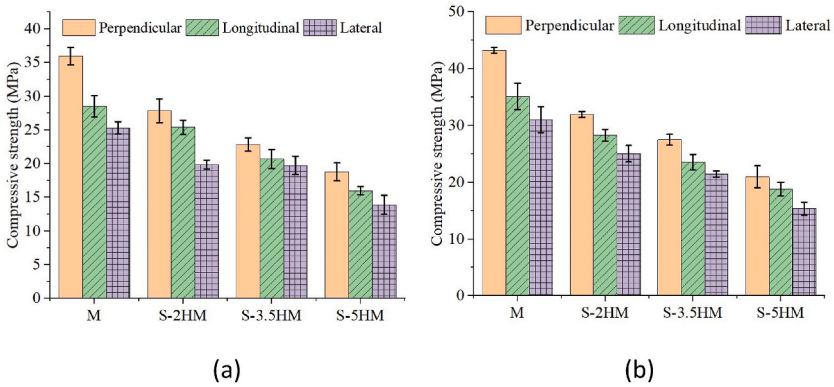

Fig. 13. (a) 7 and (b) 28-day compressive strength of the printed specimens developed using mixes under investigation.

encapsulated sodium silicate as buildability enhancing additives.

Similar to cast specimens, the compressive strength of the printed specimens reduced with the increment in the dosage of sodium silicate. At 7 days, the addition of 2 wt%, 3.5 wt%, and 5 wt% Na_2SiO_3 reduced the compressive strength by 22 %, 36 % and 47 % compared to the mix with nano clay in the perpendicular direction of loading. The reduction in compressive strength with the increment in sodium silicate dosage for longitudinal and lateral loading direction was determined as 12 % and 20 % for 2 wt% respectively, 27 % and 21 % for 3.5 wt%, 44 % and 45 % for 5 wt%. Meanwhile, in the case of 28-day-old specimens, the reduction in compressive strength with the addition of 2–5 wt% of sodium silicate was 26-19 %, 36-30 %, and 51-49 % for perpendicular, longitudinal, and lateral loading direction respectively.

At high sodium silicate dosage, the 28-day compressive strength was even lower than 20 MPa for lateral loading direction. The dissolution of sodium silicate provided equal amount of Na_2O and SiO_2 to the pore solution as the silicate modulus of the sodium silicate used is 1. The Na_2O increases the alkalinity of the pore solution which accelerates the dissolution and formation of secondary hydration products such as ettringites. The accelerated formation of ettringite increased the SYS development of the mix, however, it also caused negative impacts on the hardened properties [14]. The increment in the alkalinity of the pore solution also accelerated the dissolution of gypsum into the pore solution. According to Hamdan et al. [34], the dissolution of gypsum enriches the pore solution with Ca^{2+} and SO_4^{2-} ions, which react with sodium silicate to form C–S–H and sodium sulphates. These reaction products reduce the pH of the pore solution which in turn reduces the further dissolution of C_3S, and C_2S from cement, causing reduced compressive strength. It is worth mentioning here that there could be other attributable reasons causing the reduction of compressive strength. Nevertheless, it can be implied that the increment in sodium silicate dosage increases the buildability of the concrete, but reduces the hardened properties.

3.4.2. Interlayer bond strength

Fig. 14 shows the interlayer bond strength of the printable mixes with nano clay and various dosages of sodium silicate as buildability-enhancing additives. Similar to compressive strength results, the mix with nano clay showed higher interlayer bond strength compared to the mixes with sodium silicate. The interlayer bond strength was found to reduce with the increment in the sodium silicate dosage. For instance, the mix S-2HM (2 wt% sodium silicate dosage) exhibited an interlayer bond strength of 1.0 MPa and 1.1 MPa at 7 and 28 days respectively. The increment in the dosage of sodium silicate to 3.5 wt% (mix S-3.5HM) reduced the interlayer bond strength by 19 % and 14 % for 7 and 28 days respectively. Further increment in the sodium silicate dosage to 5 wt% (mix S-5HM) reduced the interlayer bond strength by 34 % and 35 % for 7 and 28 days respectively. This could be related to the compressive strength properties of the mixes, where the mix with nano clay showed higher compressive strength than the mixes with sodium silicate. In addition, the low interlayer bond strength for the mixes with sodium silicate can also be related to the malleability of the printed layer. As shown in Fig. 5, the stiffness of the printed layer was found to be significantly higher for the mix with sodium silicate compared to the mix with nano clay. Due to high stiffness (low malleability), the print layers fail to interlock efficiently which results in the formation of cold joints. This could also attribute to the low interlayer bond strength determined with the sodium silicate mixes. To validate this hypothesis, the volume of permeable voids was measured for both cast and printed specimens developed using mixes with nano clay and sodium silicate as shown in Fig. 15. The variation in the porosity of the printed and cast specimen relates to the interlayer and therefore was used to argue the formation of cold joints. It is known that the extrusion pressure reduces the porosity of the layer due to compaction, hence influence the difference between the porosity of a cast and printed specimen. However, it is reasonable to assume that the effect of extrusion pressure on the layer porosity should be similar for all mix designs as the mixing and printing process was maintained the same for all the mix designs.

As one can see in Fig. 15, the porosity of the mix increased with the increment in the sodium silicate dosage regardless of the specimen type (printed or cast). For instance, the pore volume of the mould cast and printed specimen for the mix M – P was determined as 7.7 % and 10.1 % respectively. For the mix with 2 wt% sodium silicate dosage, the pore volume of the cast and printed specimen was increased by 40 % and 20 % respectively. When the sodium silicate dosage was increased to 3.5 wt%, the pore volume of the cast and printed specimen was increased by 42 % and 25 % respectively. Further increment in the sodium silicate dosage increased

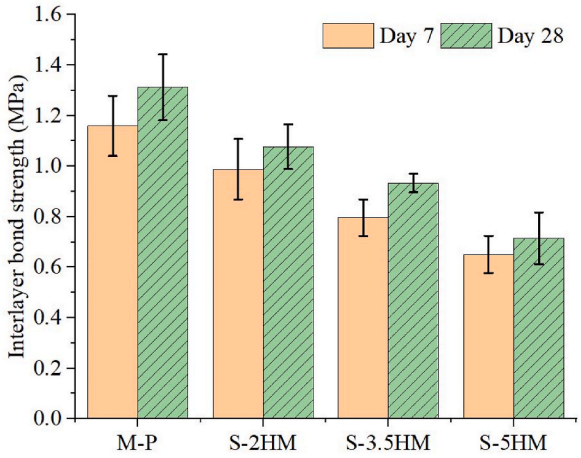

Fig. 14. Interlayer bond strength of the specimens prepared using mixes with nano clay and sodium silicate as buildability enhancing additives.

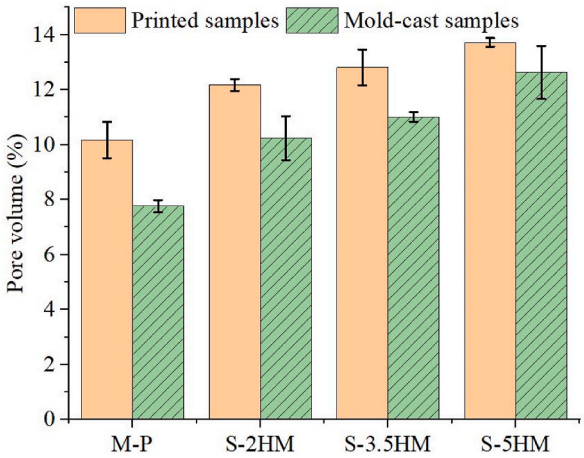

Fig. 15. The volume of permeable voids of the printed and mould-cast specimens prepared using mixes with nano clay and sodium silicate as buildability enhancing additives.

the pore volume of the cast and printed specimen by 62 % and 35 %. Furthermore, the porosity of the printed specimens was always higher than that of the cast specimens. This implies that the interlayer is more porous than the bulk of the specimen.

4. Conclusions

The buildability enhancement using encapsulated sodium silicate (set-on-demand approach) was compared with nano-clay (commonly used buildability enhancement approach) in this study. The major conclusions from this study are as follows:

1. The increment in the dosage of encapsulated sodium silicate had a negligible effect on the pumpability of the concrete as initial flow diameters for 2 % and 5 % dosage of additive were 206 mm and 174 mm respectively. That is only a 15 % reduction in the flow diameter when increasing the encapsulated sodium silicate content from 2 % to 5 %. However, after the print head heating and mixing, the static yield strength (SYS) of the concrete at 25 min increased by 221 %.
2. The buildability enhancement using encapsulated sodium silicate was significantly higher than the thixotropic additive (nano-clay). However, the hardened properties of the mix with encapsulated sodium silicate were lower than the mix with nano clay. For instance, SYS at 25 min of mixes M − P and M-5HM were 8 kPa and 122 kPa, however, the 7 days compressive strength of 3D printed specimen in the longitudinal direction were 36 MPa and 18.8 MPa respectively.
3. For 3D printed and mould-cast specimens, the mixes containing encapsulated sodium silicate displayed a high apparent volume of permeable voids (AVPV). Printed specimens consistently had a larger porosity than cast specimens. For example, the porosity of the mould cast specimens for the mix M − P and S-5HM were 7.7 % and 12.6 %, respectively. However, the printed specimen's porosity for the same mixes were 10.2 % and 13.7 %, respectively.
4. The investigated set-on-demand approach was validated using prototype printing. It was found that the mix with encapsulated sodium silicate sustained up to 41 layers, whereas the mix with nano clay failed at only 11 layers.

5. The release of the accelerator after print head heating was observed using white cement and dyed accelerator. The converted grayscale image was further processed to obtain the diffusion coefficient by fitting the Darcy equation.

CRediT authorship contribution statement

Sasitharan Kanagasuntharam: Writing – original draft, Investigation, Formal analysis, Data curation, Conceptualization. **Sayanthan Ramakrishnan:** Writing – review & editing, Visualization, Supervision, Methodology, Funding acquisition, Conceptualization. **Jay Sanjayan:** Writing – review & editing, Validation, Supervision, Resources, Project administration, Methodology, Conceptualization.

Declaration of competing interest

The authors declare that they have no known competing financial interests or personal relationships that could have appeared to influence the work reported in this paper.

Data availability

Data will be made available on request.

Acknowledgement

The authors gratefully acknowledge the financial support from the Australian Research Council Discovery Early Career Researcher Award of DE190100646 for the research work reported in this paper.

References

[1] S. Muthukrishnan, et al., Effect of Microwave Heating on Interlayer Bonding and Buildability of Geopolymer 3D Concrete Printing, 265, 2020 120786.
[2] L. Shao, et al., A novel method for improving the printability of cement-based materials: controlling the releasing of capsules containing chemical admixtures, Cement Concr. Compos. 128 (2022) 104456.
[3] F. Boscaro, et al., Eco-friendly, set-on-demand digital concrete, 3D Print. Addit. Manuf. 9 (1) (2022) 3–11.
[4] S. Muthukrishnan, S. Ramakrishnan, J. Sanjayan, Technologies for improving buildability in 3D concrete printing, Cement Concr. Compos. 122 (2021) 104144.
[5] Y. Tao, et al., Twin-pipe pumping strategy for stiffening control of 3D printable concrete: from transportation to fabrication, Cement Concr. Res. 168 (2023) 107137.
[6] L. Reiter, et al., Setting on demand for digital concrete–Principles, measurements, chemistry, validation, Cement Concr. Res. 132 (2020) 106047.
[7] S. Bhattacherjee, M. Santhanam, Investigation on the effect of alkali-free aluminium sulfate based accelerator on the fresh properties of 3D printable concrete, Cement Concr. Compos. 130 (2022) 104521.
[8] S. Ramakrishnan, S. Kanagasuntharam, J. Sanjayan, In-line activation of cementitious materials for 3D concrete printing, Cement Concr. Compos. 131 (2022) 104598.
[9] S. Kanagasuntharam, S. Ramakrishnan, J. Sanjayan, Investigating PCM encapsulated NaOH additive for set-on-demand in 3D concrete printing, Cement Concr. Compos. 145 (2024) 105313.
[10] S. Kanagasuntharam, S. Ramakrishnan, J. Sanjayan, Set-on demand concrete by activating encapsulated accelerator for 3D printing, in: RILEM International Conference on Concrete and Digital Fabrication, Springer, 2022.
[11] L. Shao, et al., A Novel Method for Improving the Printability of Cement-Based Materials: Controlling the Releasing of Capsules Containing Chemical Admixtures, 128, 2022 104456.
[12] N. Makul, et al., Microwave-assisted heating of cementitious materials: relative dielectric properties, mechanical property, and experimental and numerical heat transfer characteristics 37 (8) (2010) 1096–1105.
[13] N. Makul, et al., Applications of Microwave Energy in Cement and Concrete–A Review, 37, 2014, pp. 715–733.
[14] T. Qi, et al., Predictive hydration model of Portland cement and its main minerals based on dissolution theory and water diffusion theory 14 (3) (2021) 595.
[15] Y. Tao, et al., Stiffening Control of Cement-Based Materials Using Accelerators in Inline Mixing Processes: Possibilities and Challenges, 119, 2021 103972.
[16] G. Ma, et al., Mechanical anisotropy of aligned fiber reinforced composite for extrusion-based 3D printing, Construct. Build. Mater. 202 (2019) 770–783.
[17] AS3972, General Purpose and Blended Cements, Standards Australia, 2010.
[18] S. Guo, et al., Delaying the hydration of Portland cement by sodium silicate: setting time and retarding mechanism, Construct. Build. Mater. 205 (2019) 543–548.
[19] S.T. Witzleben, Acceleration of Portland cement with lithium, sodium and potassium silicates and hydroxides, Mater. Chem. Phys. 243 (2020) 122608.
[20] V. Ramachandran, Accelerators, in: Concrete Admixtures Handbook, Elsevier, 1996, pp. 185–285.
[21] S. Muthukrishnan, S. Ramakrishnan, J. Sanjayan, Effect of alkali reactions on the rheology of one-part 3D printable geopolymer concrete, Cement Concr. Compos. 116 (2021) 103899.
[22] D. Lootens, et al., Yield stress during setting of cement pastes from penetration tests, Cement Concr. Res. 39 (5) (2009) 401–408.
[23] S. Muthukrishnan, et al., Set on Demand Geopolymer Using Print Head Mixing for 3D Concrete Printing, 128, 2022 104451.
[24] R. Jayathilakage, P. Rajeev, J. Sanjayan, Yield stress criteria to assess the buildability of 3D concrete printing, Construct. Build. Mater. 240 (2020) 117989.
[25] ASTM, ASTM C1437, Standard Test Method for Flow of Hydraulic Cement Mortar, 2007.
[26] C. Liu, et al., Anisotropic mechanical properties of extrusion-based 3D printed layered concrete, J. Mater. Sci. 56 (30) (2021) 16851–16864.
[27] T. Marchment, et al., Interlayer strength of 3D printed concrete: influencing factors and method of enhancing, in: 3D Concrete Printing Technology, Elsevier, 2019, pp. 241–264.
[28] S. Muthukrishnan, S. Ramakrishnan, J. Sanjayan, Rapid early age strength development of in-line activated geopolymer for concrete 3D printing, Construct. Build. Mater. 406 (2023) 133312.
[29] B. Won, et al., Effects of water exposure on the interfacial bond between an epoxy resin coating and a concrete substrate 12 (22) (2019) 3715.
[30] A. Aït–Mokhtar, O. Amiri, S.J. Sammartinot, Analytic modelling and experimental study of the porosity and permeability of a porous medium—application to cement mortars and granitic rock 51 (6) (1999) 391–396.
[31] C. Zhou, et al., Deterioration of Concrete Fracture Toughness and Elastic Modulus under Simulated Acid-Sulfate Environment, 176, 2018, pp. 490–499.

[32] A. Kaboudan, M. Naderi, M.A. Afshar, The Efficiency of Darcy and Two-Dimensional Diffusion Flow Models to Estimate Water Penetration into Concrete, 34, 2021 102012.
[33] A.R. Arunothayan, et al., Development of 3D-printable ultra-high performance fiber-reinforced concrete for digital construction, Construct. Build. Mater. 257 (2020) 119546.
[34] A. Hamdan, et al., The Intrinsic Role of Network Modifiers (Ca versus Mg) in the Reaction Kinetics and Microstructure of Sodium Silicate-Activated CaO-MgO-Al2O3-SiO2 Glasses, 164, 2023 107058.